



Article

# Preparation and In Vitro Testing of Brinzolamide-Loaded Poly Lactic-Co-Glycolic Acid (PLGA) Nanoparticles for Sustained Drug Delivery

Ann-Marie Ako-Adounvo <sup>†</sup> and Pradeep K. Karla <sup>\*,†</sup>

Department of Pharmaceutical Sciences, Howard University, College of Pharmacy, Washington, DC 20059, USA

\* Correspondence: pkarla@howard.edu

<sup>†</sup> These authors contributed equally to this work.

**Abstract:** Glaucoma therapy aims at lowering intra-ocular pressure (IOP). Brinzolamide, a carbonic anhydrase inhibitor, is utilized as a second-line medication for treating ocular hypertension and primary open-angle glaucoma (POAG). The drug lowers the IOP making it a therapeutic agent against glaucoma, and due to its poor water solubility, is commercially available as Azopt<sup>®</sup>, a 1% ophthalmic suspension. Adverse effects such as blurred vision, ocular irritation, discomfort, and bitter taste are associated with the use of the marketed brinzolamide formulation. This study aims to test the feasibility of formulating and in vitro testing of brinzolamide-PLGA nanoparticles for improved toxicity profile. The nanoparticles were prepared by the oil-in-water (O/W) emulsion-solvent evaporation method. Particle size and zeta potential were determined by dynamic light scattering (DLS). The morphology of the nanoparticles was determined by scanning electron microscopy (SEM). Encapsulation of the drug was verified by high-performance liquid chromatography (HPLC) and the compatibility of the polymer and drug was verified by Fourier transform infrared (FTIR) spectroscopy. The in vitro drug release profile was assessed employing the dialysis method. Intracellular localization of the nanoparticles was assessed by confocal microscopy utilizing Rhodamine 123-loaded nanoparticles. Cytotoxicity of the formulation was assessed on Statens Serum Institut Rabbit Cornea (SIRC) and transfected Human Corneal Epithelial (SV40 HCEC) cell lines. The particle size of the nanoparticle formulations ranged from 202.3 ± 2.9 nm to 483.1 ± 27.9 nm for blank nanoparticles, and 129.6 ± 1.5 nm to 350.9 ± 8.5 nm for drug-loaded nanoparticles. The polydispersity of the formulations ranged from 0.071 ± 0.032 to 0.247 ± 0.043 for blank nanoparticles, and 0.089 ± 0.028 to 0.158 ± 0.004 for drug-loaded nanoparticles. Drug loading and encapsulation efficiencies ranged from 7.42–15.84% and 38.93–74.18%, respectively. The in vitro drug release profile for the optimized formulation was biphasic, with a ~54% burst release for the initial 3 h, followed by a cumulative 85% and 99% released at 24 and 65 h, respectively. Uptake study showed nanoparticles (NPs) localization in the cytoplasm and around the nuclei of the cells. Brinzolamide-PLGA nanoparticles were successfully developed, characterized, and tested in vitro. Preliminary data show intracellular localization of the nanoparticles in the cytoplasm of SIRC and SV40 HCEC cells. The formulations appeared to be relatively non-cytotoxic to the cells. The research data from the study provided preliminary data for successful development and promising in vitro absorption efficacy for brinzolamide-loaded PLGA nanoparticle formulation.



**Citation:** Ako-Adounvo, A.-M.; Karla, P.K. Preparation and In Vitro Testing of Brinzolamide-Loaded Poly Lactic-Co-Glycolic Acid (PLGA) Nanoparticles for Sustained Drug Delivery. *J. Clin. Transl. Ophthalmol.* **2024**, *2*, 1–14. <https://doi.org/10.3390/jcto2010001>

Academic Editor: Jack V. Greiner

Received: 28 March 2023

Revised: 28 December 2023

Accepted: 3 January 2024

Published: 9 January 2024



**Copyright:** © 2024 by the authors. Licensee MDPI, Basel, Switzerland. This article is an open access article distributed under the terms and conditions of the Creative Commons Attribution (CC BY) license (<https://creativecommons.org/licenses/by/4.0/>).

**Keywords:** brinzolamide; PLGA nanoparticles; cytotoxicity; SIRC; SV40 HCEC; ocular delivery

## 1. Introduction

Glaucoma is an incurable eye disease characterized by blindness and an increase in intraocular pressure (IOP). According to the World Health Organization (WHO), glaucoma is the second leading global cause of irreversible blindness if left untreated [1]. It is estimated that over 3.0 million Americans have glaucoma. However, only 50 percent of

this number are aware they have the condition [2]. Progression of the disease and loss of vision can be reduced with adequate medication, surgery, or both.

The disease is characterized by an increase in IOP, which over time, results in damage to retinal ganglion cells leading to blindness. The goal of current glaucoma therapies is to lower intra-ocular pressure (Figure 1). Current topically administered anti-glaucoma medications can be grouped into five main categories based on their chemical structure and pharmacological mode of action. The categories include  $\beta$ -blockers, prostaglandin analogues, miotics, carbonic anhydrase inhibitors, and  $\alpha$ -agonists [3]. These can also be used in combination.

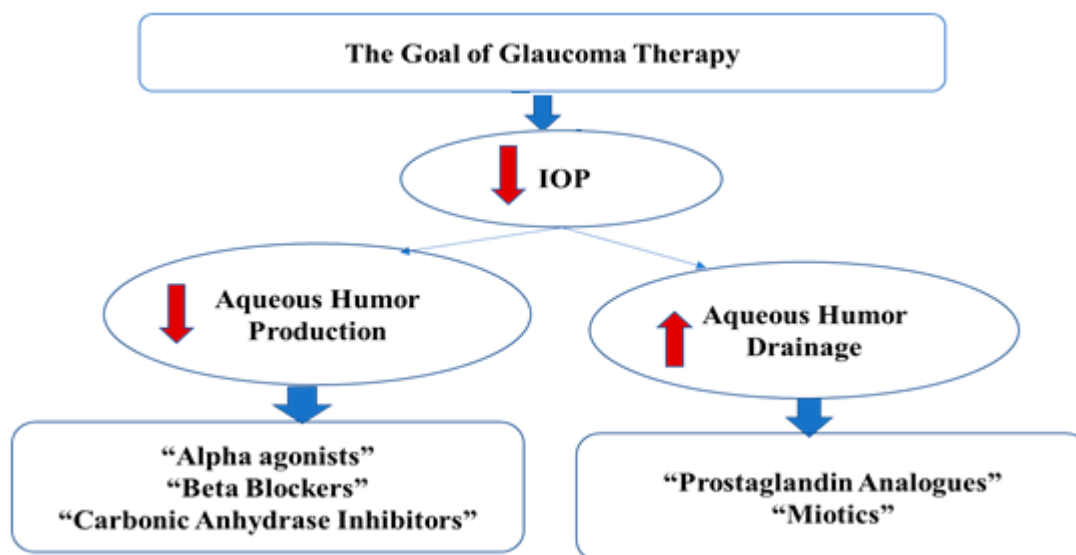
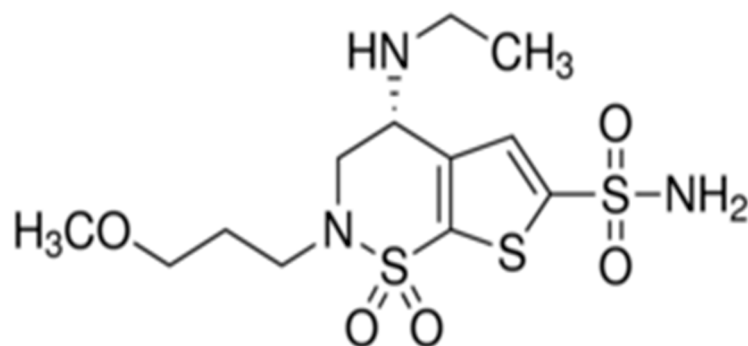


Figure 1. Glaucoma disease pathology and treatment.

Topically administered anti-glaucoma medications are often preferred and most widely used [4]. It is estimated that about 90% of all marketed ophthalmic formulations are accounted for by topically administered solution eye drops, ointments, and suspensions [5–7]. Of these, solution eye drops alone account for about 63% of all ophthalmic dosage forms [8]. Ocular medications administered topically, however, encounter many physiological barriers. The cornea is known to be the primary barrier in this route of drug administration [8]. Topically administered ocular formulations are often prone to drainage from the cul-de-sac of the eye, tear dilution, and poor permeation through the lipophilic cornea epithelia and tight junctions, thereby resulting in reduced pre-corneal drug concentrations and reduced drug absorption [9]. It is estimated that the amount of drug that can penetrate the cornea after topical administration is in the range of ~1–10% of the administered dose [4,10–12]. In addition, side effects such as dry eyes, blurred vision, eye irritation and discomfort, eye redness, eyelid edema, iris discoloration, a feeling of fatigue and bitter taste among others are experienced with topical administration. Increased doses of drugs required in topical formulations to help improve bioavailability have often resulted in an increased risk of corneal toxicity and systemic transfer of the drug [13]. Hence, there is a need for ophthalmic formulations that offer prolonged precorneal residence time for optimal drug absorption and sustained drug release.

Brinzolamide (Figure 2), a carbonic anhydrase inhibitor (CAI), is used as a second-line medication for the treatment of ocular hypertension and primary open-angle glaucoma (POAG) [14,15]. Studies have shown the drug to be effective at lowering intra-ocular pressure (IOP) [16,17]. However, due to its poor water solubility, brinzolamide is currently available on the market only as Azopt<sup>®</sup>, a 1% ophthalmic suspension (Alcon Laboratories, Ft. Worth, TX, USA). Studies have shown adverse events such as blurred vision and ocular irritation, discomfort, and a bitter taste associated with the use of the marketed brinzolamide formulation.



**Figure 2.** Chemical structure of brinzolamide.

In recent years, nanotechnology has been widely investigated for topical ophthalmic drug delivery [18,19]. Nanosystems such as liposomes, micelles, nanosuspensions, nanoemulsions, solid lipid nanoparticles, polymeric nanoparticles, hydrogels, and dendrimer have all been extensively researched for their application in ocular drug delivery. These colloidal carrier systems have particle sizes ranging from 10 nm to 1  $\mu$ m in diameter.

The objective of this study was to formulate, characterize, and test (in vitro) brinzolamide-loaded PLGA nanoparticles. PLGA is biocompatible and is well tolerated by the human body. The disadvantages of PLGA are protein binding and non-specificity with drug targeting [18]. The PLGA formulation is predicted to increase precorneal residence time, increase the absorption of brinzolamide and offer a sustained release of the drug, thereby improving ocular bioavailability and toxicity profiles. The formulation is also expected to reduce ocular irritancy.

## 2. Materials and Methods

### 2.1. Materials

Brinzolamide was purchased from United States Pharmacopeia Convention (Rockville, MD, USA). Poly (DL-lactide-co-glycolide) or (PLGA 50:50) was obtained from DURECT Corporation (Pelham, AL, USA). Ethyl Acetate, Dichloromethane and Poly (vinyl alcohol) or (PVA) of Mw ~86,000 were purchased from Acros Organics (Morris Plains, NJ, USA). Pluronic<sup>®</sup> F-68 and Poloxamer 407, HPLC Grade Acetonitrile and Methanol were obtained from Sigma-Aldrich (St. Louis, MO, USA). Deionized, distilled water was obtained from EMD Millipore Corporation (Cincinnati, OH, USA). Rhodamine 123 (Rho-123) was purchased from Marker Gene Tech, Inc. (Eugene, OR, USA). CellTox Green Cytotoxicity Assay was a gift from Promega Corporation (Madison, WI, USA). CellMask<sup>™</sup> Deep Red Plasma Membrane stain and Hoechst<sup>®</sup> 33342 were purchased from Life Technologies (Carlsbad, CA, USA).

### 2.2. Preparation of Blank, Rhodamine-Loaded, and Brinzolamide-Loaded PLGA Nanoparticles

Brinzolamide-PLGA nanoparticles were prepared by the oil-in-water (O/W) emulsion-solvent evaporation method. Briefly, brinzolamide (10–30 mg) and PLGA 50:50 (100–200 mg) were dissolved in Ethyl acetate to form the organic phase. Additional batches of nanoparticles were prepared employing Dichloromethane as a solvent. The organic phase was then added slowly and dropwise to a test tube containing the aqueous phase (a surfactant solution of either polyvinyl alcohol (PVA) or Pluronic F-68) under high-speed vortexing. The emulsion was immediately sonicated (Vibra Cell; Model VC 750; Sonics and Material Inc., Newton, CT, USA) for four bursts of 10 s on an iced water bath. The resulting nanoemulsion was immediately poured into a beaker containing excess aqueous phase (surfactant solution) and stirred at 700 rpm at ambient temperature for four hours to facilitate the evaporation of the solvent, leaving the solid nanoparticles in the aqueous phase. After solvent evaporation, the nanoparticles were separated from the surfactant solution by centrifugation (Eppendorf centrifuge 5304 R) at 11,000 rpm, 4 °C, for 60 min. The nanoparticle pellets were washed three times by re-suspending in 15 mL deionized,

distilled water and centrifuged at 11,000 rpm at 4 °C for 40 min each time to remove excess surfactant. The nanoparticles were re-dispersed in approximately 10 mL of deionized, distilled water and kept overnight in a –70 °C freezer followed by lyophilization using a laboratory-scale freeze-dryer (Labconco Corporation, Kansas City, MO, USA) for 48 h to obtain free-flowing nanoparticles. The same procedure was employed in preparing the blank and Rhodamine-123 loaded PLGA nanoparticles. In the case of Rho-123-loaded PLGA nanoparticles, the fluorescent dye (Rhodamine 123) was used in place of the drug. The freeze-dried nanoparticles were stored at 4 °C until further studies, typically within two weeks of preparation.

### 3. Characterization of the Prepared PLGA Nanoparticles

#### 3.1. Particle Size Distribution and Zeta Potential

Employing dynamic light scattering (DLS), particle size distribution was analyzed with Brookhaven 90Plus Particle Size Analyzer (Brookhaven Instruments, Holtsville, NY, USA) at a scattering angle of 90 degrees and at a temperature of 25 °C. The zeta potential of the nanoparticles in suspension was also measured using the ZetaPlus Zeta Potential Analyzer (Brookhaven Instruments, NY). Each nanoparticle suspension was assessed in triplicate, and the values obtained for particle size analysis and zeta potential were reported as mean ± SD.

#### 3.2. Scanning Electron Microscopy (SEM)

The morphology of the prepared nanoparticles was examined by JEOL JSM-7600F Field Emission Scanning Electron Microscope (JEOL USA Inc., Peabody, MA, USA). Small aliquots of various dilutions of the nanoparticle suspensions were placed on disc-shaped carbon tapes mounted onto aluminum stubs. The samples were then dried under vacuum (Vacuum Oven 285; Fisher Scientific, Hampton, NH, USA), followed by sputter coating with gold metal using the Hummer (Technics Inc., Alexandria, VA, USA) prior to visualization by scanning electron microscope under vacuum, at 20 kV and a 12 mm working distance.

#### 3.3. Fourier Transform Infrared (FTIR) Spectroscopy

FTIR spectra were obtained for brinzolamide (pure drug), blank PLGA nanoparticles and brinzolamide-loaded PLGA nanoparticles using the Perkin Elmer Spectrum 100 FT-IR Spectrometer (PerkinElmer, Downers Grove, IL, USA). Samples were scanned at 4 mm/s over a region of 650–4000  $\text{cm}^{-1}$ .

### 4. HPLC Analysis

High-performance liquid chromatography (HPLC) was used to determine drug loading and to quantify the amount of brinzolamide released from the nanoparticles. A validated HPLC method per USP Monograph (USP29–NF24, Brinzolamide) was used with slight modification [20]. Mobile phase A: triethylamine (TEA) phosphate buffer was prepared by diluting 4 ml TEA in 1000 mL deionized, distilled water (DDI) and adjusting it to pH 3.0 with ortho-phosphoric acid. Mobile phase B was HPLC grade acetonitrile. The mobile phases (A and B) were premixed at a ratio of 80:20 (buffer: acetonitrile), filtered through a 0.22  $\mu\text{m}$  bottle-top filter, and degassed for 40 min in a Branson 2510 Ultrasonic Bath.

A Shimadzu LC Solutions Chromatography Data System (Shimadzu Scientific Instruments, Columbia, MD, USA) was used in this study. The system was composed of a system controller (SCL-10A VP), pumps (LC-10AD VP), autosampler (SIL-10AD VP) and a photodiode array detector (SPD-M10A VP). A connected PC installed with LC solution software, version 1.2X was used to record and integrate the chromatograms. An Alltech Premium EPS C18 analytical column (100 Å; 150 mm × 4.6 mm; 5  $\mu\text{m}$ ) was employed as the solid phase in the separation of brinzolamide. Standard curve for brinzolamide was prepared with drug concentrations ranging from 1 to 100  $\mu\text{g}/\text{mL}$ . The elution was carried out isocratically at a flow rate of 0.8 mL/minute, sample injection volume was 20  $\mu\text{L}$ , and the detection wavelength was set at 254 nm.

## 5. Drug Loading (%DL) and Encapsulation Efficiency (%EE)

To estimate drug loading, 10 mg of lyophilized brinzolamide-PLGA nanoparticles were dissolved in 5 mL ethyl acetate by vortexing and sonication. The sample solutions were filtered through 0.22  $\mu\text{m}$  Durapore (PVDF) membrane filter and the filtrate was analyzed by HPLC. This was carried out in triplicate. Brinzolamide concentrations were estimated from the resultant peak AUC values using the pre-plotted standard calibration curve for brinzolamide. Drug loading of the formulation batches was calculated as per Equation (1). The process efficiency or the amount of drug encapsulated was estimated as in Equation (2).

$$\%DL = (\text{Amount of drug in NPs} \div \text{Weight of NPs}) \times 100 \quad (1)$$

$$\%EE = \frac{(\text{Total amount of drug in NPs}) \times 100}{\text{Amount of Drug used in NPs preparation}} \quad (2)$$

## 6. In Vitro Drug Release Studies

In vitro release profile of brinzolamide from the prepared nanoparticles was assessed by quantifying the cumulative amount of drug in the release medium over time. Briefly, a weight of brinzolamide-PLGA nanoparticles equivalent to 1 mg of drug was dispersed in 1 mL of freshly prepared simulated tears 2, pH 7.4 (0.2% *w/v* sodium bicarbonate; 0.008% *w/v* calcium chloride; 0.67% *w/v* sodium chloride; distilled deionized water) [21]. The nanoparticle suspension was transferred into a pre-wetted Spectra/Por molecular porous membrane dialysis tubing (MWCO 12–14 kD) and placed into a 50 mL centrifuge tube containing 20 mL of release medium (simulated tears with 0.1% *v/v* Tween 80). The centrifuge tube was placed into a rotator oven set to 37 °C and 50 rotations per minute. At pre-selected time intervals, 1.0 mL sample was withdrawn from the release medium and replaced with an equal volume of fresh medium to maintain sink conditions. The samples withdrawn at each time interval were analyzed by HPLC (as described above under HPLC analysis), and the cumulative amount of drug released from the nanoparticles over time was calculated.

## 7. Cytotoxicity Studies of the Nanoparticle Formulation

### 7.1. Cell Cultures

Staten Serum Institut Rabbit Cornea (SIRC) cell line was obtained from American Type Culture Collection (ATCC) (Manassas, VA, USA). SV40-immortalized human corneal epithelial cell line (SV40 HCEC) was also obtained as a kind gift from Dr. Alison McDermott (University of Houston, College of Optometry, Houston, TX, USA).

Cells were cultured as per established standard protocols [22]. Briefly, the cells were grown in T-75 culture flasks and maintained in ATCC's Eagle's Minimum Essential Medium (EMEM) supplemented with 10% *v/v* heat-inactivated fetal bovine serum (FBS). The SV40-immortalized human corneal epithelial cells (SV40 HCEC) were also grown in T-75 culture flasks and maintained in a 1:1 Dulbecco's Modified Eagles Medium (DMEM)-F/12 medium, supplemented with 1% *v/v* penicillin/streptomycin, 0.5% *v/v* DMSO Hybri-Max<sup>®</sup>, 0.2% *v/v* Normocin, 1.2% *v/v* HEPES, 0.01% *v/v* epidermal Growth Factor, 0.01% *v/v* Cholera Toxin, and 0.0005% *v/v* insulin. In addition, 10% *v/v* FBS was added to the medium in the flask at the time of culturing. Both SIRC and SV40 HCEC were maintained as a monolayer at 37 °C in a balanced air incubator with a humidified atmosphere of 5% CO<sub>2</sub>.

### 7.2. In Vitro Cytotoxicity Assay

Cells (SIRC and SV40 HCEC) were seeded at a density of 10,000 cells/100  $\mu\text{L}$ /well, in opaque-walled 96-well plates and were allowed to attach for 24 h post-seeding. The cells were treated with Blank PLGA nanoparticles, pure brinzolamide suspension, and brinzolamide-PLGA nanoparticles equivalent to 1% brinzolamide. The cells were exposed to the treatments for 72 h. Because the assay measures loss of cell membrane integrity, toxicity control cells were included in the wells that were treated with lysis solution to

represent 100% kill or 100% toxicity. CellTox Green Cytotoxicity Assay was added and further incubated for 15 min, followed by fluorescence measurement at Ex: 485 nm, Em: 520 nm using CytoFluor® Multi-well Plate Reader Series 4000 (PerSeptive Biosystems, Framingham, MA, USA).

### 8. In Vitro Intracellular Localization of Nanoparticles

SIRC and SV40 HCEC cells were seeded in glass-bottom microwell dishes (MatTek Corp., Ashland, MA, USA) at a density of 600,000 cells/dish/1.5 mL medium. After allowing the cells to attach for 24 h, the medium was replaced with rhodamine-123-loaded nanoparticles suspended in culture medium (2.0 mg/mL), and the cells were further incubated for 6 h post-treatment. At 5 h post treatment, Hoechst® 33342 was added to cells to counterstain the nuclei. At 6 h post treatment, cells were thoroughly washed with PBS, to remove the nanoparticles that were not internalized. Thereafter, CellMask™ Deep Red was added to counterstain the plasma membrane for 30 min. Fluorescent images were captured using a Nikon Ti-E-PFS inverted Spinning-disk confocal scanning microscope equipped with a 60X 1.4NA Plan Apo Lambda Objective. The system was outfitted with a self-contained 4-line laser module (excitation at 405, 488, 561, and 640 nm), and Andor iXon 897 EMCCD camera. Confocal and DIC images acquired were processed using the NIS-Element software (Nikon Instrument Inc., Melville, NY, USA) and Adobe Photoshop CS5 software.

Statistical Analysis: Experiments were performed with a minimum of  $n = 3$  ( $n = 6$  for data in Figure 8), and the results are expressed as the mean  $\pm$  SD. Statistical significance testing was performed with a two-factor analysis of variance (ANOVA; SPSS, ver. 29.0; SPSS Inc., Chicago, IL, USA). The difference between mean values was considered significant at  $p \leq 0.05$ . The Fisher least significance difference (LSD) method was used to discriminate between significant differences among the mean values.

### 9. Results and Discussion

#### 9.1. Physicochemical Characterization of BNZ-Loaded PLGA Nanoparticles: Particle Size and Zeta Potential Analysis

Ocular barriers are often characterized by tight junctions. To increase penetration through ocular tissues, the particle size of nanoparticle formulations is an important parameter to consider [23–26]. In this study, the hydrodynamic particle size and polydispersity measured by dynamic light scattering (DLS) for the formulations ranged from 202.3 nm  $\pm$  2.9 to 483.1 nm  $\pm$  27.9 for blank nanoparticles, and 129.6 nm  $\pm$  1.5 to 350.9 nm  $\pm$  8.5 for drug-loaded nanoparticles (Table 1). The polydispersity of the formulations ranged from 0.071  $\pm$  0.032 to 0.247  $\pm$  0.043 for blank nanoparticles, and 0.089  $\pm$  0.028 to 0.158  $\pm$  0.004 for drug-loaded nanoparticles. The particle size distribution as assessed by DLS is shown in Figure 3. Statistical significance was assessed by considering the blank formulation (F10B) as a control.

**Table 1.** Effect of various formulation components on particle size and polydispersity. Statistical significance was measured by two-factor ANOVA. \*  $p \leq 0.05$ ; \*\*  $p \leq 0.01$ .

Formulation	PLGA 50:50 (mg)	Drug (mg)	Solvent (5 mL)	Surfactant	Particle Size (nm)	Polydispersity
F1	100	-	Ethyl acetate	0.8% PVA	271.1 $\pm$ 4.3 **	0.112 $\pm$ 0.027 *
F2	100	-	Ethyl acetate	1.0% F-68	254.9 $\pm$ 2.9 **	0.107 $\pm$ 0.018 *
F3	100	-	Ethyl acetate	1.2% F-68	297.7 $\pm$ 12.8 **	0.117 $\pm$ 0.051 *
F4	100	-	Ethyl acetate	1.0% PVA	327.8 $\pm$ 10.9 **	0.325 $\pm$ 0.012 **
F5	100	-	Dichloromethane	2.0% PVA	483.1 $\pm$ 27.9 *	0.247 $\pm$ 0.043 **
F6	100	-	Ethyl acetate	1.2% F-68/1.0% PVA	271.7 $\pm$ 1.8 **	0.107 $\pm$ 0.012 *
F7	100	-	Ethyl acetate	1.0% PVA/1.2% F-68	276.1 $\pm$ 2.9 **	0.167 $\pm$ 0.021 **
F8	100	-	Ethyl acetate	2.5% PVA	310.3 $\pm$ 3.8 **	0.167 $\pm$ 0.024 **
F9	100	-	Ethyl acetate	1.5% PVA	284.9 $\pm$ 3.9 **	0.134 $\pm$ 0.018 **
F10	100	-	Ethyl acetate	1.5% F-68	208.7 $\pm$ 3.4	0.075 $\pm$ 0.012
F10B	200	-	Ethyl acetate	1.5% F-68	202.3 $\pm$ 2.9	0.071 $\pm$ 0.032
BNZ001	200	20	Ethyl acetate	1.5% F-68	234.3 $\pm$ 6.8 **	0.089 $\pm$ 0.028*

Table 1. Cont.

Formulation	PLGA 50:50 (mg)	Drug (mg)	Solvent (5 mL)	Surfactant	Particle Size (nm)	Polydispersity
BNZ002	200	10	Ethyl acetate	1.5% F-68	129.6 ± 1.5	0.108 ± 0.047
BNZ003	200	20	Ethyl acetate	1.5% PVA	350.9 ± 3.4 **	0.113 ± 0.018 **
BNZ004	200	30	Dichloromethane	1.5% F-68	303.3 ± 4.9 **	0.158 ± 0.004 **
BNZ005	150	30	Ethyl acetate	1.5% F-68	130.7 ± 1.1	0.120 ± 0.012
Rho123-NP1	200	1.5 mg Rho123	Ethyl acetate	1.5% F-68	195.2 ± 1.4	0.099 ± 0.017

Note: Values represents the mean and standard deviation of three replicates.

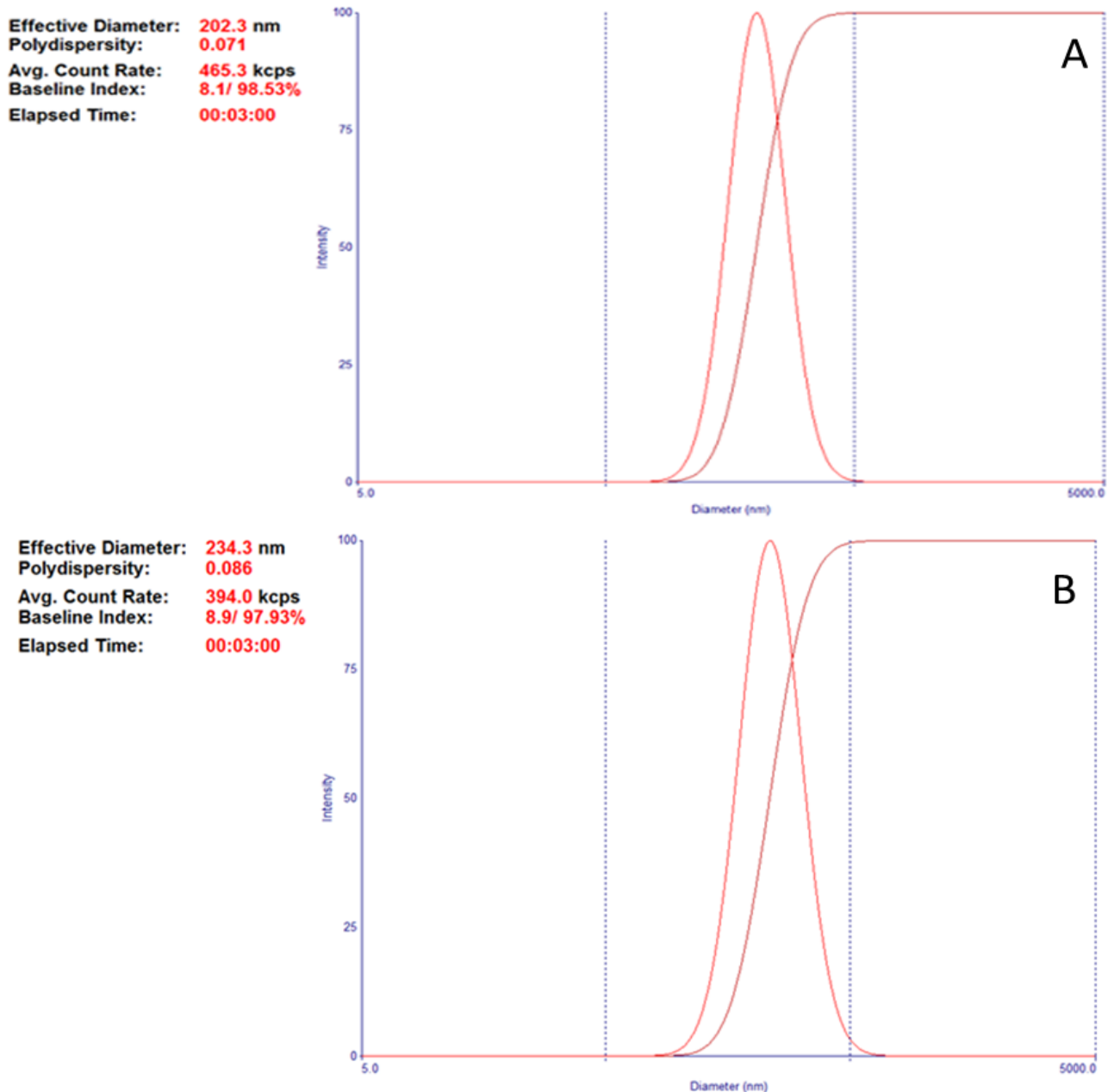


Figure 3. Size distribution of: (A) Blank PLGA NPs (Formulation F10B), (B) brinzolamide-loaded PLGA NPs (Formulation BNZ001).

It was observed that the effective diameter, encapsulation efficiency, and drug loading were affected by formulation variables such as the drug to polymer ratio and the type and concentration of the solvent and surfactant used in the formulation (Table 1). The use of Dichloromethane (DCM) in nanoparticle formulations has been shown to produce larger nanoparticle sizes [27]. This is possibly due to the increased interfacial tension of DCM compared to ethyl acetate. At 20 °C, DCM has a surface tension of 28.12 dyne/cm, whereas that of ethyl acetate is 23.75 dyne/cm [28]. Particle size and the drug to polymer ratio appeared to have an influence on drug loading. When the drug to polymer ratio was kept constant, the formulation with the larger mean effective diameter appeared to have slightly better drug loading (comparing BNZ001 and BNZ003) [28]. Additionally, it was shown that increasing the polymer to drug ratio increases encapsulation efficiency (% EE) (comparing BNZ001, BNZ002, BNZ004 and BNZ005). Drug loading (%DL) also appeared to decrease with an increase in polymer amounts (Table 2). These observations are consistent with earlier studies that examined the effect of the drug to polymer ratio on loading and encapsulation [29,30]. The zeta potential (mV) for brinzolamide-loaded PLGA nanoparticles ranged from  $-33.12 \pm 1.67$  to  $-40.73 \pm 0.53$  (Table 2). The zeta potential is an indication of the stability of the nanoparticles in suspension. Absolute zeta potential values above  $|30|$  mV are considered stable as they are less likely to flocculate in suspension as dispersed particles repel each other [31,32]. Statistical significance was assessed by comparing the formulations with an absolute zeta potential value of  $|30|$  mV as a control.

**Table 2.** Effect of various formulation components on particle size and polydispersity. Statistical significance was measured by two-factor ANOVA. \*\*  $p \leq 0.01$ .

Formulation	Drug:Polymer	Surfactant	Zeta Potential (mV)	EE (%)	DL (%)
BNZ001	1:10	1.5% F-68	$-35.21 \pm 1.52$ **	64.65	12.93
BNZ002	1:20	1.5% F-68	$-37.98 \pm 1.39$ **	74.18	7.42
BNZ003	1:10	1.5% PVA	$-33.12 \pm 1.67$ **	68.53	13.71
BNZ004	1:7	1.5% F-68	$-40.73 \pm 0.53$ **	52.80	15.84
BNZ005	1:5	1.5% F-68	$-38.57 \pm 1.02$ **	38.93	11.68

## 9.2. SEM and FTIR

Scanning electron microscopy images showed the successful formation of nanoparticles with a spherical morphology and smooth surface (Figure 4). FTIR analysis was performed to establish that the drug had been successfully encapsulated into the PLGA nanoparticle and not just adsorbed onto or mixed with the polymer. FTIR spectra obtained for pure brinzolamide showed characteristic absorption bands for S=O ( $1333.88 \text{ cm}^{-1}$  and  $1148.20 \text{ cm}^{-1}$ ), C-NH-C ( $3313.26 \text{ cm}^{-1}$ ), CH<sub>3</sub> ( $2962.70 \text{ cm}^{-1}$ ), -CH<sub>2</sub> ( $1451.50 \text{ cm}^{-1}$ ). The absorption band at  $3095.78 \text{ cm}^{-1}$  signifies a heterocyclic moiety containing sulfur and nitrogen elements as found in brinzolamide [33]. The characteristic absorption band for PLGA observed at  $1750 \text{ cm}^{-1}$  and  $1752 \text{ cm}^{-1}$  for blank PLGA and drug-loaded PLGA nanoparticles, respectively, is attributed to the carbonyl group (C=O) found in the monomers. Also, absorption at  $1087.35 \text{ cm}^{-1}$  in the PLGA nanoparticle is indicative of the presence of C-O of aliphatic polyesters [34]. The spectra for the pure drug and the drug-loaded PLGA nanoparticles were non-superimposable, suggesting that preparation did not result in a physical mixture but that the drug was indeed entrapped in the nanoparticle core (Figure 5). Drug entrapment in nanoparticles was further analyzed by HPLC.

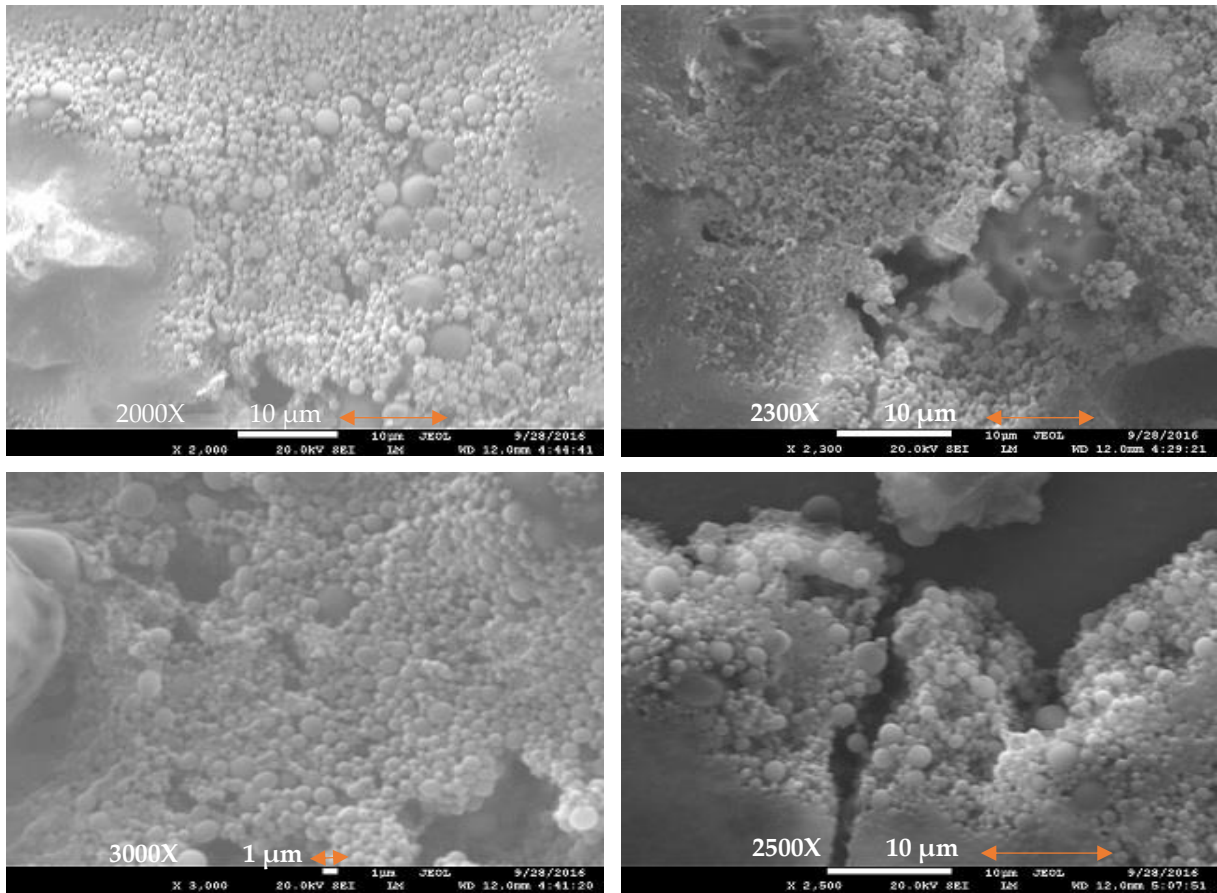


Figure 4. Typical SEM images of freeze-dried brinzolamide-loaded PLGA nanoparticles (BNZ004) at various magnifications.

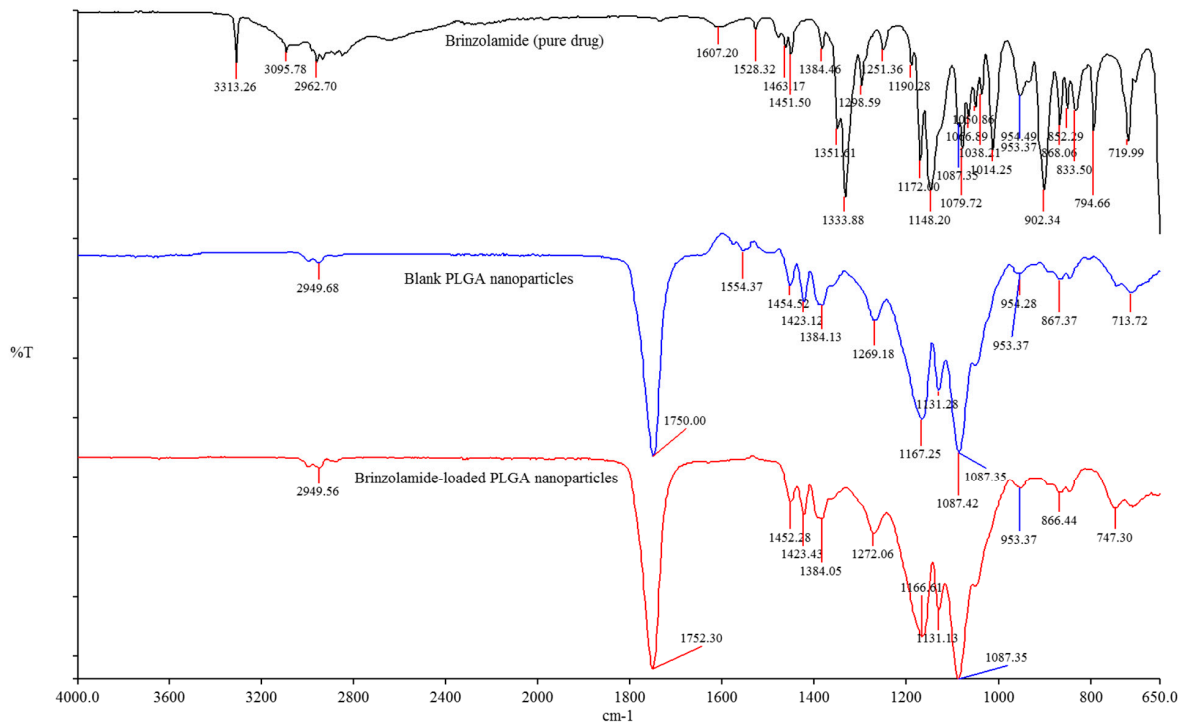
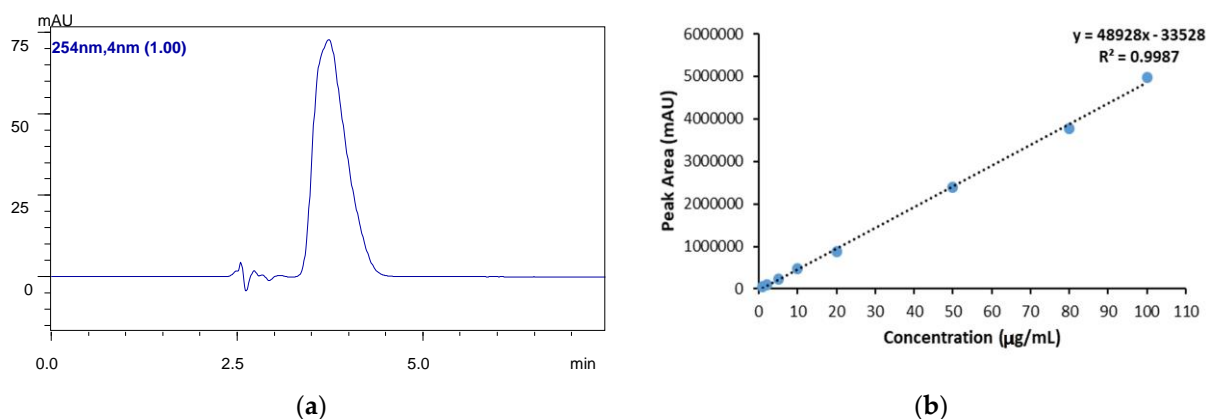


Figure 5. FTIR spectra of pure drug, blank PLGA nanoparticles, and drug-loaded PLGA nanoparticles (BNZ004).

### 9.3. In Vitro Release Study

The standard calibration curve generated by the high-pressure liquid chromatography method employed for the quantification of brinzolamide was found to be linear over a concentration range of 1–100  $\mu\text{g}/\text{mL}$ , with a correlation coefficient of 0.9987 (Figure 6). The average retention time was  $3.7 \text{ min} \pm 0.004$ . Drug loading for the formulations ranged between 7.42 and 15.84% (Table 2). The formulation employing 100 mg PLGA did not yield a detectable drug loading, and hence the drug loading data were presented for formulations employing 150 mg and 200 mg PLGA. Based on particle size, encapsulation efficiency and drug loading, formulation BNZ004 was found to be the most optimum. In vitro release of brinzolamide from BNZ004 was determined in simulated tear fluid (pH 7.4). A 1 mL sample collected from the 50 mL corresponds to 2% of the medium, and the volume may not accurately represent the sink conditions, as most of the drug remains in the surrounding liquid. To minimize the error and ensure uniformity, the samples were collected immediately after pausing the rotator oven. Figure 7 shows the in vitro release profile of brinzolamide from the nanoparticles. As shown in Figure 7, the formulation demonstrated initial rapid release with 54% of the drug in 3 h. This was followed by slower release, resulting in drug accumulation of  $\sim 60\%$  in 16 h. This second phase had a slower rate of drug release for an extended duration of time, resulting in  $\sim 85\%$  of the encapsulated drug being released in 24 h (Figure 7). Nearly 100% drug release was observed at 65 h. PLGA was widely utilized in the development of multiple ophthalmic and other drug delivery systems. The common release mechanism is attributed to the degradation rate of PLGA. Further, based on the formulation type, aspects such as solubilization, penetration of water, erosion followed by diffusion of PLGA fragments, and the rate of drug release were known to affect the release mechanism [35]. Hence, the release mechanism can be complex, making it difficult to accurately interpret the reasons for variations in the release profiles. Our subsequent studies will perform comprehensive mathematical modeling of brinzolamide-PLGA nanoparticles formulation to understand the release mechanism.



**Figure 6.** (a) HPLC chromatogram of brinzolamide. (b) Calibration curve of brinzolamide.

### 9.4. Cytotoxicity Study

The cytotoxicity of optimized brinzolamide-PLGA nanoparticles formulation was tested on two well-established corneal epithelial cell lines, SIRC and SV40 HCEC, using the CellTox Green Cytotoxicity Assay. The assay measures changes in cell membrane integrity as a result of cell death. By binding DNA in cells that have lost their membrane integrity (dead cells), the fluorescence property of the assay dye is greatly enhanced [36–42]. Pure brinzolamide suspension was used as a standard for comparison (Figure 8). Data suggest that the brinzolamide-loaded PLGA nanoparticle formulation is safe on both rabbit (SIRC) and human (SV40 HCEC) corneal epithelial cell lines at a fixed brinzolamide concentration of 0.01 g/mL (1% brinzolamide). In addition, when compared to the pure brinzolamide suspension, the drug-loaded PLGA nanoparticles exhibited a better safety profile in both cell lines (Figure 8). PLGA is considered safe by the US FDA and is widely employed

as biomaterial in many drug delivery systems [6]. Therefore, using the data obtained for the blank PLGA nanoparticles as reference, the percentage difference in cell viability was estimated for the brinzolamide-loaded nanoparticles (~1.9% and 1.5% in SIRC and SV40 HCEC, respectively).

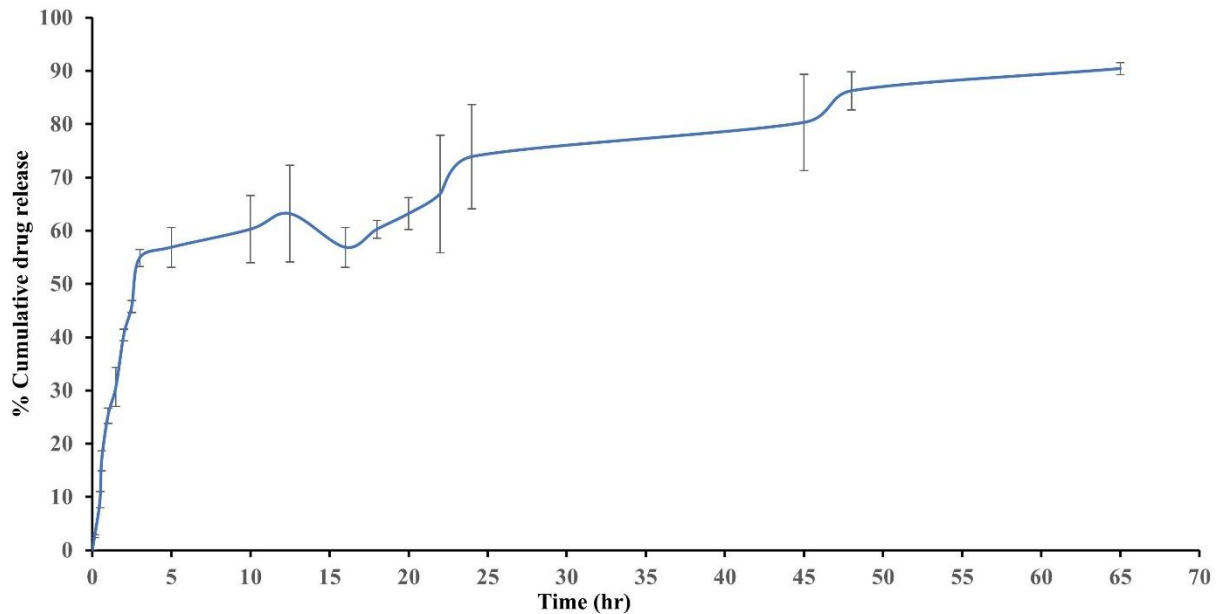


Figure 7. Drug release profile of optimized formulation BNZ004 (N = 3, mean ± Stdev).

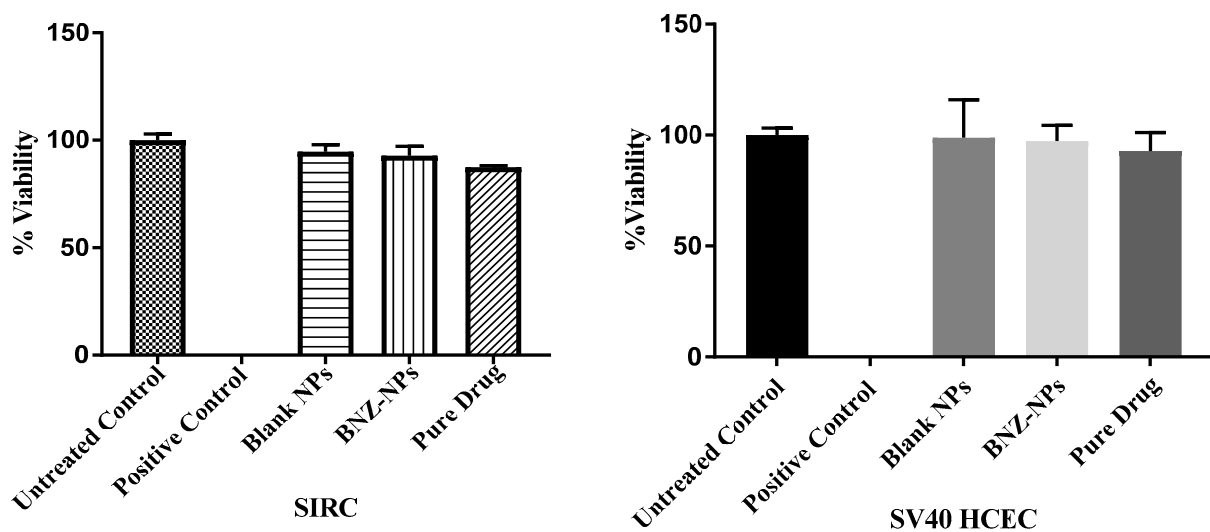
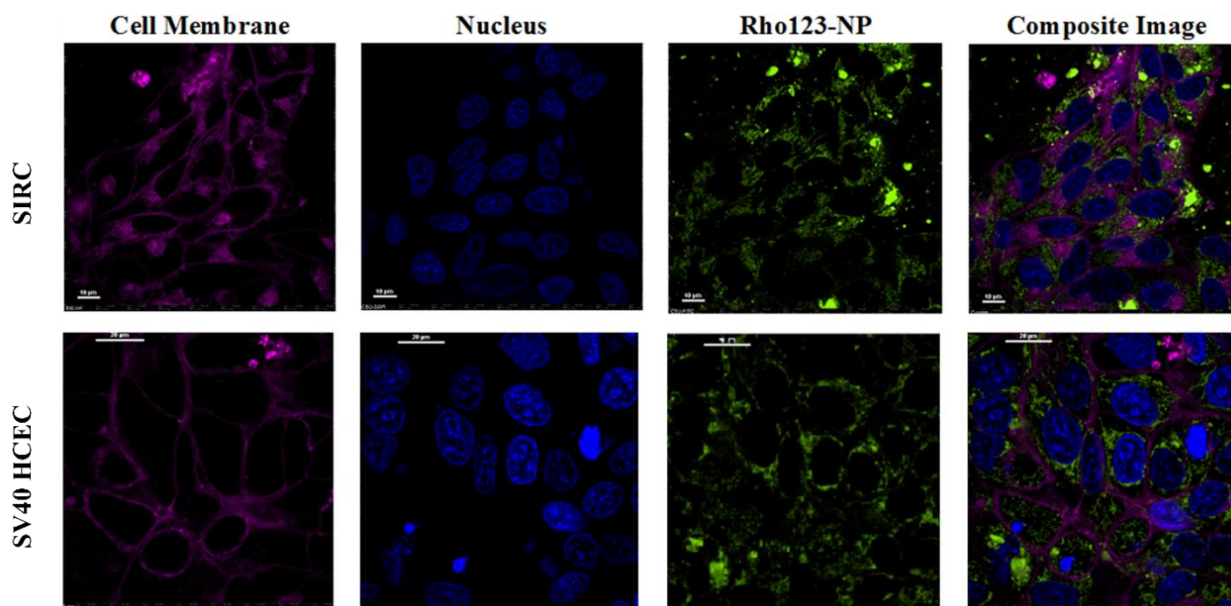


Figure 8. Cytotoxicity study of blank PLGA NPs, positive control (Lysis Solution), Brinzolamide-PLGA NPs (BNZ004) and pure drug suspension. Statistical significance was measured by two-factor ANOVA.

### 9.5. Cellular Uptake Study

Nanoparticles encapsulating fluorescent dye, Rhodamine 123, were used to study the cellular uptake and intracellular localization of nanoparticles [35–41]. The confocal images obtained clearly showed the rhodamine-loaded PLGA nanoparticles (observed as green color) being taken up by both cell lines (Figure 9). The green nanoparticles observed between the cell membrane (stained red) and the nuclei (stained blue with DAPI), suggest localization of the nanoparticles in the cytoplasm around the nuclei of the cells.



**Figure 9.** Confocal images showing intracellular localization of nanoparticles.

## 10. Conclusions

In this study, brinzolamide-loaded PLGA nanoparticles were successfully prepared employing the oil-in-water emulsification-solvent evaporation method. Different formulations were experimented with, to optimize particle size, polydispersity, and drug loading. Formulations employing dichloromethane (DCM) as a solvent and polyvinyl alcohol (PVA) as a stabilizer resulted in nanoparticles with larger effective diameters, whereas those utilizing ethyl acetate and Pluronic F-68 produced nanoparticles with smaller effective diameters and polydispersity index. The zeta potential values ( $>30$  mV) indicated a stable emulsion. The SEM data indicated the formation of spherical and smooth brinzolamide-loaded nanoparticles. The FTIR analysis confirmed the encapsulation of the drug by the nanoparticles. Drug release from the nanoparticles appeared to be diphasic. The formulation demonstrated an initial rapid release that can be attributed to the drug being located in the outermost matrix and adsorbed onto the surface of the PLGA nanoparticles. This was followed by a slower diffusion-controlled release. The release profile was heterogeneous. This can be attributed to the formulation variables (or) the release kinetic approach utilized in the current study, where a small sample was collected for release analysis, instead of replacing the entire release media to create the perfect sink conditions. Cytotoxicity data demonstrated that brinzolamide-loaded PLGA nanoparticle formulation was well tolerated by both rabbit and human cornea epithelial cell lines. This confocal imaging demonstrated superior absorption of nanoparticles by the corneal epithelial cells. Further, the cellular uptake data indicated the formation of an intracellular drug depot that provides a sustained drug release. The research data from the study provided preliminary data for successful development and promising *in vitro* absorption efficacy for brinzolamide-loaded PLGA nanoparticle formulation. Future studies will focus on stability assessment, drug release kinetics mathematical model analysis, and *in vivo* efficacy assessment of brinzolamide-loaded PLGA nanoparticle formulation.

**Author Contributions:** The research work for performed by A.-M.A.-A. and supervised by P.K.K. All authors have read and agreed to the published version of the manuscript.

**Funding:** This work was partly supported with funds from the BRIDGE Research Grant, Bristol Myers Squibb (BMS) Research Grant (PI: Pradeep Karla) and RCMI Research Grant (PI: William Southerland). The Howard University Research Centers in Minority (RCMI) Program is supported by the National Institute on Minority Health and Health Disparities (NIMHD) of the National Institutes

of Health (NIH) under Award Number 2U54MD007597. The content is solely the responsibility of the authors and does not necessarily represent the official views of the National Institutes of Health.

**Institutional Review Board Statement:** Not applicable.

**Informed Consent Statement:** We provide consent for the publication of this research article along with the data/figures and contributing author details.

**Data Availability Statement:** The authors state that the data supporting the conclusions from the manuscript are made available within the manuscript as figures and tables.

**Acknowledgments:** The authors are thankful to Anna Allen and Ruby Boateng, Department of Biology for their help with operating confocal microscope and the acquisition of fluorescent images, and James Griffin and Anthony Gomez, HU Nanoscale Science & Engineering Facility, for their help with the operation of splatter coater and scanning electron microscope.

**Conflicts of Interest:** There is no conflict of interest with the proposed work.

## References

1. Resnikoff, S.; Pascolini, D.; Etya'ale, D.; Kocur, I.; Pararajasegaram, R.; Pokharel, G.P.; Mariotti, S.P. Global data on visual impairment in the year 2002. *Bull. World Health Organ.* **2004**, *82*, 844–851. [PubMed]
2. Glaucoma Research Foundation. *Glaucoma Facts and Stats*; Glaucoma Research Foundation: San Francisco, CA, USA, 2016.
3. Migdal, C. What therapy to use in glaucoma? In *Ophthalmology*, 2nd ed.; Yanoff, M., Duker, J.S., Eds.; Mosby: Boston, MA, USA, 2004; pp. 1539–1543.
4. Dey, S.; Patel, J.; Anand, B.; Jain-Vakkalagadda, B.; Kaliki, P.; Pal, D.; Ganapathy, V.; Mitra, A. Molecular evidence and functional expression of P-glycoprotein (MDR1) in human and rabbit corneal epithelial cell lines. *Investig. Ophthalmol. Vis. Sci.* **2003**, *44*, 2909–2918. [CrossRef] [PubMed]
5. Lang, J. Ocular drug delivery conventional ocular formulations. *Adv. Drug Deliv. Rev.* **1995**, *16*, 39–43. [CrossRef]
6. Bourlais, C.; Acar, L.; Zia, H.; Sado, P.; Needham, T.; Leverage, R. Ophthalmic drug delivery systems—Recent advances. *Prog. Retin. Eye Res.* **1998**, *17*, 33–58. [CrossRef] [PubMed]
7. Negarsenker, M.; Londhe, V.; Nadkarni, G. Preparation and evaluation of liposomal formulations of tropicamide for ocular delivery. *Int. J. Pharm.* **1999**, *190*, 63–71. [CrossRef] [PubMed]
8. Sieg, J.; Robinson, J. Mechanistic studies on transcorneal penetration of pilocarpine. *J. Pharm. Sci.* **1976**, *65*, 1816–1822. [CrossRef]
9. Gaudana, R.; Ananthula, H.; Parenky, A.; Mitra, A. Ocular drug delivery. *AAPS J.* **2010**, *12*, 348–360. [CrossRef]
10. Urtti, A. Challenges and obstacles of ocular pharmacokinetics and drug delivery. *Adv. Drug Deliv. Rev.* **2006**, *58*, 1131–1135. [CrossRef]
11. Lapalus, P.; Moulin, G.; Fredj, D. Kinetics of drugs in ophthalmology. *Bull. Soc. D'ophtalmologie Fr.* **1985**, *1*, 31–48.
12. Schoenwald, R.D. Ocular pharmacokinetics. In *Textbook of Ocular Pharmacology*; Lippincott-Raven, Zimmerman, T.J., Kooner, K.S., Sharir, M., Fechtner, R.D., Eds.; Lippincott Williams & Wilkins: Philadelphia, PA, USA, 1997; Volume 9, pp. 119–138.
13. Labetoulle, M.; Frau, E.; Jeunne, C.L. Systemic adverse effects of topical ocular treatments. *Presse Med.* **2005**, *34*, 589–595. [CrossRef]
14. Iester, M. Brinzolamide ophthalmic suspension: A review of its pharmacology and use in the treatment of open angle glaucoma and ocular hypertension. *Clin. Ophthalmol.* **2008**, *2*, 517–523. [CrossRef] [PubMed]
15. Lee, D.A.; Higginbotham, E.J. Glaucoma and its treatment: A review. *Am. J. Health-Syst. Pharm.* **2005**, *62*, 691–699. [CrossRef] [PubMed]
16. Wang, T.H.; Huang, J.Y.; Hung, P.T.; Shieh, J.W.; Chen, Y.F. Ocular hypotensive effect and safety of brinzolamide ophthalmic solution in open angle glaucoma patients. *J. Formos. Med. Assoc.* **2004**, *103*, 369–373. [PubMed]
17. March, W.F.; Ochsner, K.I. The long-term safety and efficacy of brinzolamide 1.0% (azopt) in patients with primary open-angle glaucoma or ocular hypertension. The Brinzolamide Long-Term Therapy Study Group. *Am. J. Ophthalmol.* **2000**, *129*, 136–143. [CrossRef]
18. Sharma, O.P.; Patel, V.; Mehta, T. Nanocrystal for ocular drug delivery: Hope or hype. *Drug Deliv. Transl. Res.* **2016**, *6*, 399–413. [CrossRef]
19. Liu, S.; Jones, L.; Gu, F.X. Nanomaterials for ocular drug delivery. *Macromol. Biosci.* **2012**, *12*, 608–620. [CrossRef]
20. USP29—NF24, Brinzolamide. Available online: [http://www.pharmacopeia.cn/v29240/usp29nf24s0\\_m10206.html](http://www.pharmacopeia.cn/v29240/usp29nf24s0_m10206.html) (accessed on 20 March 2016).
21. Marques, M.; Loebenberg, R.; Almukainzi, M. Simulated Biological Fluids with Possible Application in Dissolution Testing. *Dissolution Technol.* **2011**, *18*, 15–28. [CrossRef]
22. Toropainen, E.; Ranta, V.; Vellonen, K.; Palmgren, J.; Talvitie, A.; Laavola, M.; Suhonen, P.; Hamalainen, K.M.; Auriola, S.; Urtti, A. Paracellular and passive transcellular permeability in immortalized human corneal epithelial cell culture model. *Eur. J. Pharm. Sci.* **2003**, *20*, 99–106. [CrossRef]

23. Nagai, N.; Ono, H.; Hashino, M.; Ito, Y.; Okamoto, N.; Shimomura, Y. Improved corneal toxicity and permeability of tranilast by the preparation of ophthalmic formulations containing its nanoparticles. *J. Oleo Sci.* **2014**, *63*, 177–186. [[CrossRef](#)]
24. Gupta, H.; Aqil, M.; Khar, R.K.; Ali, A.; Bhatnagar, A.; Mittal, G. Sparfloxacin-loaded PLGA nanoparticles for sustained ocular drug delivery. *Nanomedicine* **2010**, *6*, 324–333. [[CrossRef](#)]
25. Guinedi, A.S.; Mortada, N.D.; Mansour, S.; Hathout, R.M. Preparation and evaluation of reverse-phase evaporation and multilamellar niosomes as ophthalmic carriers of acetazolamide. *Int. J. Pharm.* **2005**, *306*, 71–82. [[CrossRef](#)] [[PubMed](#)]
26. Patravale, V.B.; Date, A.A.; Kulkarni, R.M. Nanosuspension: A promising drug delivery strategy. *J. Pharm. Pharmacol.* **2004**, *56*, 827–840. [[CrossRef](#)] [[PubMed](#)]
27. Sahana, D.K.; Mittal, G.; Bhardwaj, V.; Kumar, M.N. PLGA nanoparticles for oral delivery of hydrophobic drugs: Influence of organic solvent on nanoparticle formation and release behavior in vitro and in vivo using estradiol as a model drug. *J. Pharm. Sci.* **2008**, *97*, 1530–1542. [[CrossRef](#)] [[PubMed](#)]
28. Görner, T.; Gref, R.; Michenot, D.; Sommer, F.; Tran, M.N.; Dellacherie, E. Lidocaine-loaded biodegradable nanospheres. I. Optimization Of the drug incorporation into the polymer matrix. *J. Control. Release* **1999**, *57*, 259–268. [[CrossRef](#)] [[PubMed](#)]
29. Biswal, I.; Dinda, A.; Mohanty, S.; Dhara, M.; Das, D.; Chowdary, K.A.; Si, S. Influence of Drug/Polymer Ratio on the Encapsulation Efficiency of Highly Hydrophilic Drug. *Asian J. Chem.* **2011**, *23*, 1973–1978.
30. Pavanveena, C.; Kavitha, K.; Anil, K.S.N. Formulation and evaluation of trimetazidine hydrochloride loaded chitosan microspheres. *Int. J. Appl. Pharm.* **2010**, *2*, 11–14.
31. Park, J.H.; Jeong, H.; Hong, J.; Chang, M.; Kim, M.; Roy, S.; Chuck, R.S.; Lee, J.K.; Park, C.Y. The Effect of Silica Nanoparticles on Human Corneal Epithelial Cells. *Sci. Rep.* **2016**, *6*, 37762. [[CrossRef](#)]
32. Heurtault, B.; Saulnier, P.; Pech, B.; Proust, J.E.; Benoit, J.P. Physico-chemical stability of colloidal lipid particles. *Biomaterials* **2003**, *24*, 4283–4300. [[CrossRef](#)]
33. Li, H.; Liu, Y.; Zhang, Y.; Fang, D.; Xu, B.; Zhang, L.; Chen, T.; Ren, K.; Nie, Y.; Yao, S.; et al. Liposomes as a Novel Ocular Delivery System for Brinzolamide: In Vitro and In Vivo Studies. *AAPS PharmSciTech* **2016**, *17*, 710–717. [[CrossRef](#)]
34. Marques, D.R.; Dos Santos, L.A. Analysis of Poly(Lactic-co-Glycolic Acid)/Poly(Isoprene) Polymeric Blend for Application as Biomaterial. *Polímeros* **2013**, *23*, 579–584. [[CrossRef](#)]
35. Hines, D.J.; Kaplan, D.L. Poly (lactic-co-glycolic acid) controlled release systems: Experimental and modeling insights. *Crit. Rev. Ther. Drug Carr. Syst.* **2013**, *30*, 257–276. [[CrossRef](#)] [[PubMed](#)]
36. Chiaraviglio, L.; Kirby, J.E. Evaluation of Impermeant, DNA-Binding Dye Fluorescence as a Real-Time Readout of Eukaryotic Cell Toxicity in a High Throughput Screening Format. *ASSAY Drug Dev. Technol.* **2014**, *12*, 219–228. [[CrossRef](#)] [[PubMed](#)]
37. Wu, W.; Li, J.; Wu, L.; Wang, B.; Wang, Z.; Xu, Q.; Xin, H. Ophthalmic delivery of brinzolamide by liquid crystalline nanoparticles: In vitro and in vivo evaluation. *AAPS PharmSciTech* **2013**, *14*, 1063–1071. [[CrossRef](#)]
38. Chakole, C.M.; Sahoo, P.K.; Pandey, J.; Chauhan, M.K. A green chemistry approach towards synthesizing hydrogel for sustained ocular delivery of brinzolamide: In vitro and ex vivo evaluation. *J. Indian Chem. Soc.* **2022**, *99*, 100323. [[CrossRef](#)]
39. Anwar, M.; Muhammad, F.; Akhtar, B. Biodegradable nanoparticles as drug delivery devices. *J. Drug Deliv. Sci. Technol.* **2021**, *64*, 102638. [[CrossRef](#)]
40. Rodrigo, M.; Garcia-Herranz, D.; Aragon-Navas, A.; Subias, A.; Martinez-Rincon, T.; Mendez-Martinez, S.; Cardiel, M.J.; Garcia-Fejoo, J.; Ruberte, J.; Herrero-Vanrell, R.; et al. Long-term corticosteroid-induced chronic glaucoma model produced by intracameral injection of dexamethasone-loaded PLGA microspheres. *Drug Deliv.* **2021**, *28*, 2427–2446. [[CrossRef](#)]
41. Yang, F.; Cabe, M.; Nowak, H.A.; Langert, K.A. Chitosan/poly(lactic-co-glycolic)acid Nanoparticle Formulations with Finely-Tuned Size Distributions for Enhanced Mucoadhesion. *Pharmaceutics* **2022**, *14*, 95. [[CrossRef](#)]
42. Shao, X.; Wei, Z.; Song, X.; Hao, L.; Cai, X.; Zhang, Z.; Peng, Q.; Lin, Y. Independent effect of polymeric nanoparticle zeta potential/surface charge, on their cytotoxicity and affinity to cells. *Cell Prolif.* **2015**, *48*, 465–474. [[CrossRef](#)]

**Disclaimer/Publisher’s Note:** The statements, opinions and data contained in all publications are solely those of the individual author(s) and contributor(s) and not of MDPI and/or the editor(s). MDPI and/or the editor(s) disclaim responsibility for any injury to people or property resulting from any ideas, methods, instructions or products referred to in the content.